Proceedings 10th NUMGE 2023
10th European Conference on Numerical Methods in Geotechnical Engineering
Zdravković L, Konte S, Taborda DMG, Tsiampousi A (eds)
ISSN

doi: 10numge-2023-123-Gao

Nonlocal regularization of an anisotropic critical state model for sand

Z.W. Gao[1*], X. Li[1] and D.C. Lu[2]
[1]*James Watt School of Engineering, University of Glasgow, Glasgow, G12 8QQ, UK*
[2]*Key Laboratory of Urban Security and Disaster Engineering of Ministry of Education, Beijing University of Technology, Beijing 100124, China*
[*]*Corresponding author: Email: zhiwei.gao@glasgow.ac.uk; Tel: +44 1413303927*

ABSTRACT: Many advanced constitutive models which can capture the strain-softening and state-dependent dilatancy response of sand have been developed. These models can give a good prediction of the single soil element behaviour under various loading conditions. But the solution will be highly mesh-dependent when they are used in real boundary value problems due to the strain-softening. They can give mesh-dependent strain localization patterns and bearing capacity of foundations on sand. Nonlocal regularization of an anisotropic critical state sand model is presented. The evolution of void ratio which has a significant influence on strain-softening is assumed to depend on the volumetric strain increment of both the local and neighbouring integration points. The nonlocal model has been used in simulating both drained and undrained plane strain compression. In plane strain compression, mesh-independent results for the force-displacement relationship and shear band thickness can be obtained when the mesh size is smaller than the internal length. The regularization method is thus proper for application in practical geotechnical engineering problems.

Keywords: Sand anisotropy; critical state; nonlocal theory; mesh dependency; strain localization

1 INTRODUCTION

Many advanced constitutive models for sand have been developed (Jefferies, 1993; Li and Dafalias 2000, 2002; Dafalias et al., 2004; Gao et al., 2014; Yao et al., 2017, 2019, 2020; Tian et al., 2017). These models can capture the state-dependent dilatancy and strain-softening of single sand elements under various loading conditions. But a sand model with strain-softening can give highly mesh-dependent results when used in finite element analysis of real boundary value problems. For instance, the model gives a non-unique force and displacement relationship for plane strain compression on dense sand with strain localization (Galavi and Schweiger, 2010; Mallikarachchi and Soga, 2020). The computed thickness and orientation of shear bands are also mesh-dependent. The shear band thickness decreases as the element size decreases and the shear band direction may follow the direction of element edges (Galavi and Schweiger, 2010). When a sand model with strain-softening is used in practical boundary value problems, the solution can become unreliable due to the mesh-dependency. For instance, the bearing capacity predicted by a strain-softening sand model can change dramatically when the mesh size and orientation change (Loukidis and Salgado, 2011; Chaloulos et al., 2019). The mesh-dependency is caused by the assumption used in standard elastoplastic models that the stress-strain relationship at an integration point is dependent on the local stress, strain and state variables only.

Many methods for regularizing the mesh-dependence of finite element solutions of strain-softening models have been developed, including the nonlocal theories (Eringen, 1972; Bažant and Gambarova, 1984; Galavi and Schweiger, 2010; Mallikarachchi and Soga, 2020), viscous plasticity (Oka et al., 1995; Di Prisco et al., 2002), strain-gradient plasticity (Arsenlis and Parks, 1999; Chambon et al., 2001; Huang et al., 2004) and mico-polar theories (Chang and Ma, 1991; Tordesillas and Walsh, 2002; Tejchman and Wu, 2010). These methods can significantly reduce the mesh sensitivity of the finite element solutions. In particular, the nonlocal method is found effective and convenient in regularizing strain-softening models for soils (Galavi and Schweiger, 2010; Mallikarachchi and Soga, 2020; Di Prisco and Imposimato, 2003; Summersgill et al. 2017, 2018; Mánica et al., 2018). In a fully nonlocal constitutive model, the stress, strain and state variables should all be considered as nonlocal variables. Since a fully nonlocal model makes the constitutive equations complex, the partially nonlocal approach has been used in most cases. In a partially nonlocal model, some of the state variables (e.g., plastic shear strain, void ratio or yield surface size) are assumed nonlocal (Galavi and

Schweiger, 2010). Indeed, the partially nonlocal approach is found sufficient for regularizing most soil models with strain softening.

This paper presents a method for regularizing an anisotropic critical state sand model based on the work by Mallikarachchi and Soga (2020). The paper is organized as follows. The original constitutive model and regularization method are first introduced. The nonlocal model is then used to simulate strain localization in plane strain compression. The practicality of this regularization method in real geotechnical engineering problems is discussed.

2 THE ORIGINAL CONSTITUTIVE MODEL

The model used in this study was developed based on the anisotropic critical state theory which considers the fabric evolution of sand during loading (Li and Dafalias, 2012). A detailed discussion of the model can be found in (Gao et al. 2014, 2020). This model accounts for the plastic deformation of sand under shear only. Therefore, a Mohr-Coulomb type yield function is used

$$f = R/g(\theta) - H_d = 0 \tag{1}$$

where $R = \sqrt{3r_{ij}r_{ij}/2}$, $r_{ij} = \left(\sigma_{ij} - p\delta_{ij}\right)/p$ is the stress ratio tensor, σ_{ij} is the stress tensor, $p = \sigma_{ii}/3$ is the mean effective stress, δ_{ij} is the Kronecker delta (= 1 for $i = j$, and = 0 for $i \neq j$), H_d is the hardening parameter and $g(\theta)$ is an interpolation function which describes the variation of critical state stress ratio with the Lode angle θ of r_{ij} (Li and Dafalias, 2002; Gao et al., 2014) The hardening law for the yield function is expressed as

$$dH_d = \langle L \rangle r_H \tag{2a}$$

$$r_H = \frac{Gh_1 \exp\left(h_2 A\right)}{(1+e)^2\sqrt{pp_a}R}\left[M_c g(\theta)\exp(-n\zeta) - R\right] \tag{2b}$$

where L is the loading index, $\langle \quad \rangle$ are the Macaulay brackets which make $\langle L \rangle = L$ for $L > 0$ and $\langle L \rangle = 0$ for $L \leq 0$, h_1, h_2 and n are model parameters, G is the elastic shear modulus, A is the anisotropic variable (Li and Dafalias, 2012; Gao et al., 2014), e is the void ratio, p_a is the atmospheric pressure, M_c is the critical state stress ratio in triaxial compression and ζ is the dilatancy state parameter (Li and Dafalias, 2012). This hardening law can capture the strain-softening response of dense sand. The plastic shear strain increment de_{ij}^p is expressed as

$$de_{ij}^p = \langle L \rangle m_{ij} \tag{3}$$

where $m_{ij} = \frac{\frac{\partial g}{\partial r_{ij}} - \left(\frac{\partial g}{\partial r_{mn}}\delta_{mn}\right)\delta_{ij}/3}{\left\|\frac{\partial g}{\partial r_{ij}} - \left(\frac{\partial g}{\partial r_{mn}}\delta_{mn}\right)\delta_{ij}/3\right\|}$ and g is the plastic potential function in the r_{ij} space

$$g = R/g(\theta) - H_g e^{-k_h(1-A)^2} = 0 \tag{4}$$

where k_h is a model parameter and H_g is determined based on the current stress state and A. The term involving A in Equation (4) enables the model to capture the non-coaxial response of sand caused by fabric anisotropy (Gao et al., 2013, 2014). The total plastic strain increment $d\varepsilon_{ij}^p$ as below

$$d\varepsilon_{ij}^p = de_{ij}^p + \frac{1}{3}d\varepsilon_v^p\delta_{ij} = \langle L \rangle\left(m_{ij} + \sqrt{\frac{2}{27}}D\delta_{ij}\right) \tag{5}$$

where $d\varepsilon_v^p$ is the plastic volumetric strain increment and D is the dilatancy function (Gao et al., 2020). In this model, the fabric evolution with plastic shear strain is considered

$$dF_{ij} = \langle L \rangle k_f\left(n_{ij} - F_{ij}\right) \tag{6}$$

where dF_{ij} is the increment of fabric tensor, k_f is a model parameter and n_{ij} is the loading direction defined as

$$n_{ij} = \frac{\frac{\partial f}{\partial r_{ij}} - \left(\frac{\partial f}{\partial r_{mn}}\delta_{mn}\right)\delta_{ij}/3}{\left\|\frac{\partial f}{\partial r_{ij}} - \left(\frac{\partial f}{\partial r_{mn}}\delta_{mn}\right)\delta_{ij}/3\right\|} \tag{7}$$

3 NONLOCAL FORMULATION OF THE CONSTITUTIVE MODEL

Following Mallikarachchi and Soga (2020), the increment of void ratio de is assumed to be nonlocal as below

$$de = (1 + e)d\varepsilon_{vn} \tag{8}$$

where positive de is associated with volume contraction and $d\varepsilon_{vn}$ is the nonlocal volumetric strain increment

$$d\varepsilon_{vn} = \frac{\sum_{k=1}^{N} w_i v_i d\varepsilon_{vi}}{\sum_{k=1}^{N} w_i v_i} \tag{9}$$

where N is the number of integration points within the averaging area, w_i, v_i and $d\varepsilon_{vi}$ represent the weight function, volume and local volumetric strain increment of integration point i. The weight function proposed by Galavi and Schweiger (2010) is used

$$w_i = \frac{r_i}{l^2}\exp\left(-\frac{r_i^2}{l^2}\right) \tag{10}$$

where l is the internal length, r_i is the distance between the current integration point and the i-th integration point used for calculating the averaged value in Equation (8). Note that several other weight functions have also be proposed in the literature but one in Galavi and Schweiger (2010) is found to give the best regularization results for soils with strain softening (Summersgill et al., 2018). More details can be found in Gao et al. (2021).

4 STRAIN LOCALIZATION UNDER PLANE STRAIN COMPRESSION

The strain localization under plane strain compression will be simulated by ABAQUS. The model parameters (Table 1) are the same as those in Gao et al. (2020). The sample size (60mm×120mm) and boundary conditions are shown in Figure 1.

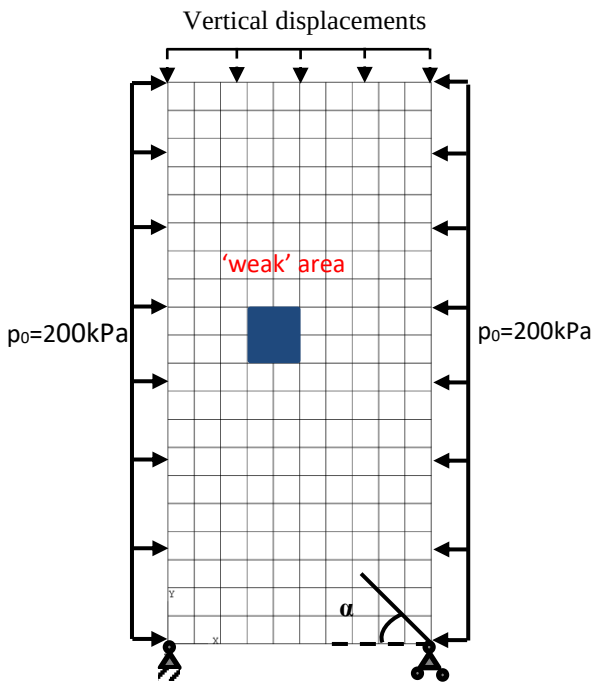

Figure 1. The boundary conditions and bedding plane orientation for the plane strain test simulations

A confining pressure of $p_0 = 200$kPa is applied on the two vertical sides. Vertical displacement is applied on the top side with the horizontal displacement unconstrained. The bottom side is pinned at the left and free to move to the right. The strain localization is triggered by assigning a 'weak' area (12mm×12mm) with inclined bedding plane orientation ($\alpha = 45°$). Horizontal bedding plane orientation ($\alpha = 0°$) is specified for the remaining area. The 8-noded plane strain elements with reduced integration are used in the simulations. The initial void ratio of the sample is $e_0 = 0.65$ (relative density $D_r = 88\%$) and the initial degree of anisotropy is $F_0 = 0.4$.

Table 1. Model parameters for Toyoura sand

Model Parameters	Value
G_0	125
ν	0.1
M_c	1.25
c	0.75
e_Γ	0.934
λ_c	0.019
ξ	0.7
n	2.0
h_1	0.45
d_1	1.0
m	3.5
k_f	0.5
e_A	0.075
k_h	0.03
h_2	0.5

The internal length l is an important parameter for nonlocal soil models, as it is used for the weight function of Equation (10). Figure 2 shows the effect of l on the $s - R_v$ relationship predicted by the nonlocal model, where s is the vertical displacement and R_v is the total vertical reaction force measure on the top surface of the sample.

The mesh size is 4mm×4mm (450 elements). The nonlocal model always gives a higher peak R_v and a slower rate of strain-softening than the local model. This is due to that the nonlocal model makes the stress and strain distribution more uniform in the soil. For the nonlocal model, the peak R_v shows little variation with l the rate of strain-softening is slower at bigger l.

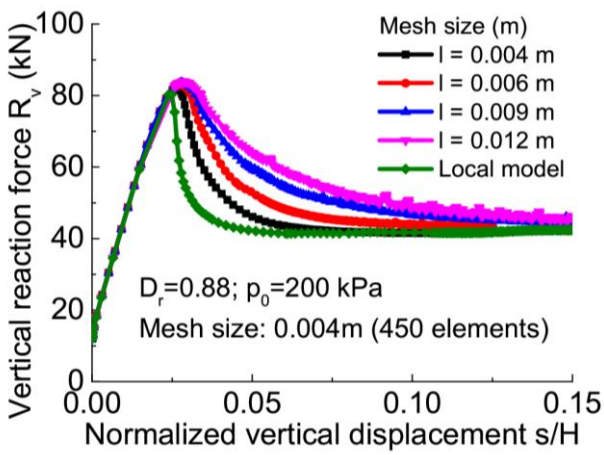

Figure 2. Effect of internal length l on the force-displacement relationship in plane strain compression

4.1 Simulation of the strain localization

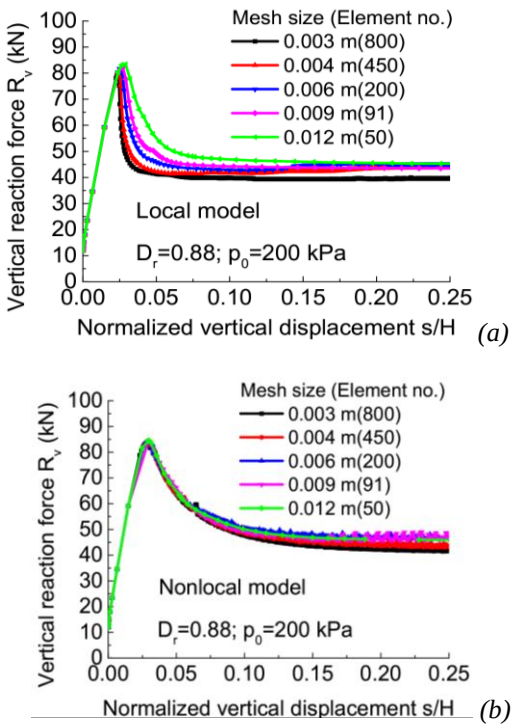

Figure 3. Force-displacement relationship predicted by the (a) original and (b) nonlocal model for drained condition

Figure 3 and Figure 4 show the $s - R_v$ relationship predicted by the local and nonlocal models with different mesh sizes. The same internal length of l =12 mm is used in both drained and undrained condition. The local model gives mesh-dependent $s - R_v$ relationship with higher peak R_v and slower rate of strain-softening at a bigger mesh size (Figure 3(a) and Figure 4(a)). The $s - R_v$ relationship predicted by the nonlocal model is insensitive to the mesh size. The visible difference can only be observed at $s > 0.1H$, where H is the initial height of the sample (Figure 3(b) and Figure 4(b)).

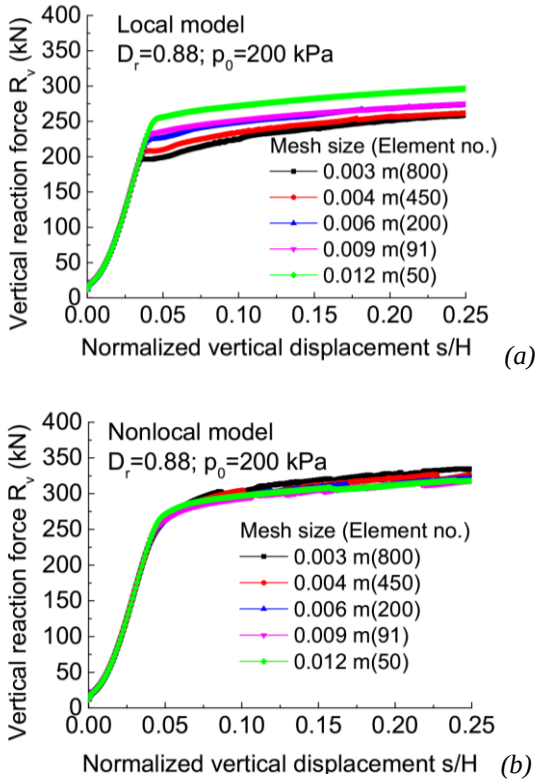

Figure 4. Force-displacement relationship predicted by the (a) original and (b) nonlocal model for undrained condition

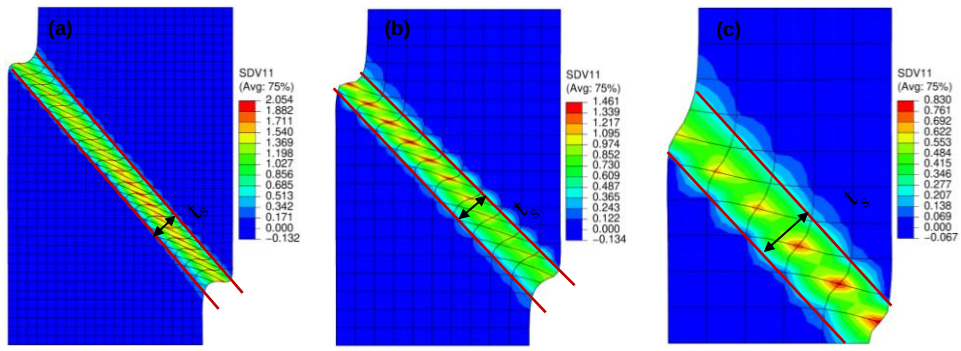

Figure 5. Shear band predicted by the nonlocal model at s/H=0.09 (a) 800 elements; (b) 200 elements and (c) 50 elements

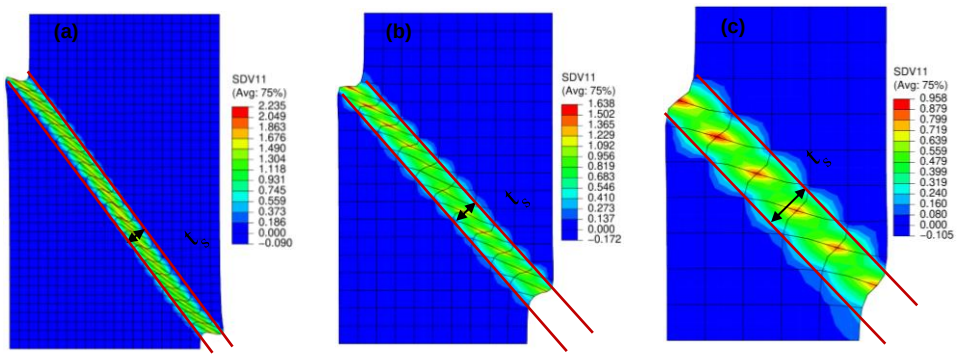

Figure 6. Shear band predicted by the local model at s/H=0.09 (a) 800 elements; (b) 200 elements and (c) 50 elements

Figure 5 and Figure 6 show the shear strain localization predicted by the local and nonlocal models under drained condition, where SDV11 represents the total shear strain. The shear band thickness t_s measured at $s = 0.09H$ for drained condition is shown in Figure 7 (a) and undrained condition in Figure 7 (b). When the mesh size $h < l$, the location and thickness of shear bands predicted by the nonlocal model are independent of the mesh size (Figure 7). When $h = l$, the shear band predicted by the nonlocal model locates at a lower position (Figure 5(c)). The shear band thickness is also close to that predicted by the local mode (Figure 7). This means that the regularization method works when $h < l$. When the mesh size is the same, the shear band thickness predicted by the nonlocal model increases with l (Figure 8). But there is not a linear relationship between h and l, which has been reported in previous research (Galavi and Schweiger, 2010). The shear band thickness predicted by the local model increases with the mesh size, which is in agreement with existing studies (Figure 8). The shear band orientation predicted by the nonlocal model varies between 47° (50 elements) and 51° (800 elements), and that predicted by the local model varies between 47° (50 elements) and 53° (800 elements) (Figure 5 and Figure 6). This indicates that the shear band orientation predicted by the nonlocal model is not sensitive to the mesh size.

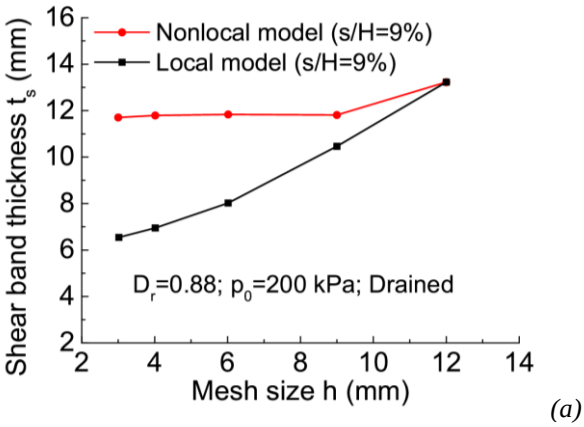

(a)

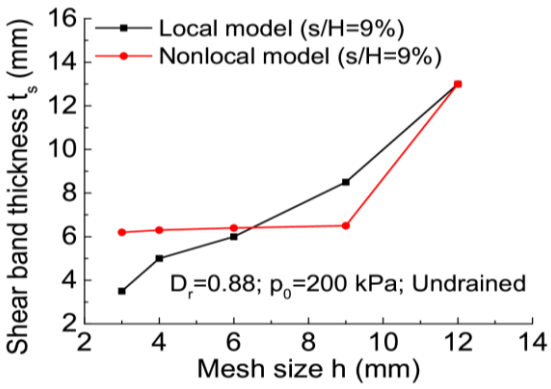

(b)

Figure 7. The effect of mesh size (a) drained and (b) undrained condition on the shear band thickness. The internal length l is 12 mm for the nonlocal model

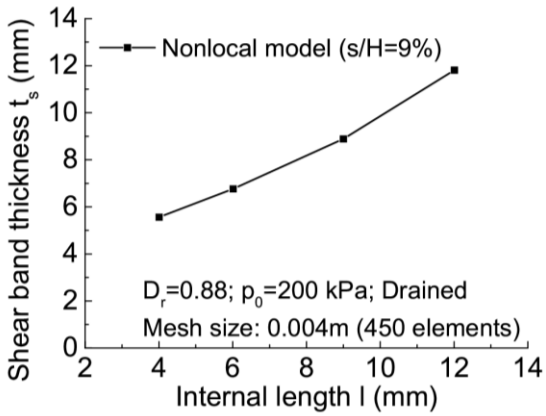

(a)

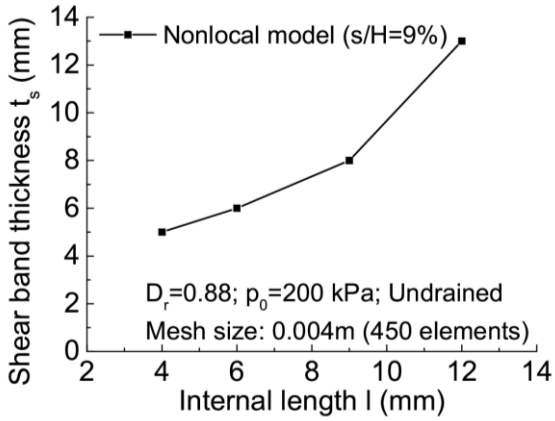

(b)

Figure 8. The effect of internal length (a) drained and (b) undrained condition on the shear band thickness. The internal length l is 12 mm for the nonlocal model

Based on these results, it can be concluded that the nonlocal model can give a mesh-independent force-displacement relationship for different mesh sizes. But mesh-independent strain localization pattern can only be observed when the mesh size is smaller than the internal length. To improve the regularization method for larger mesh sizes, more state variables which control the strain-softening (e.g., F_{ij} and H_d) should be assumed nonlocal. But this would significantly increase the model complexity and computational time, which has been discussed before.

5 CONCLUSIONS

Nonlocal regularization of an anisotropic critical state sand model is presented. The evolution of the void ratio is assumed to depend on the volumetric strain increment at the local and neighbouring integration points (Mallikarachchi and Soga, 2020). The nonlocal model has been implemented for finite element analysis using the in drained and undrained plane strain compression on the sand.

The nonlocal model gives a mesh-independent force-displacement relationship in plane strain compression with strain localization. The location and thickness of the shear band are mesh-independent when the mesh

size is smaller than the internal length. Better regularization results for the strain localization can be obtained if the two variables F_{ij} and H_d which affect the strain-softening are made nonlocal. But this would significantly increase the model complexity and the computational time. The regularization method is thus proper for solving practical geotechnical engineering problems.

6 ACKNOWLEDGEMENTS

The third author would like to acknowledge the financial support of the National Natural Science Foundation of China (No. 52025084).

REFERENCES

Arsenlis, A. Parks, D. 1999. Crystallographic aspects of geometrically-necessary and statistically-stored dislocation density, *Acta Mater* **47**, 1597-1611.

Bažant, Z., Gambarova, P. 1984. Crack Shear in Concrete: Crack Band Microplane Model, *J. Struct. Eng.* **110**, 2015-2035.

Chaloulos, Y., Papadimitriou, A., Dafalias, Y. 2019. Fabric Effects on Strip Footing Loading of Anisotropic Sand, *J. Geotech. Geoenviron. Eng.* **145**, 04019068.

Chambon, R., Caillerie, D., Matsuchima, T. 2001. Plastic continuum with microstructure, local second gradient theories for geomaterials: localization studies, *Int. J. Solid. Struct.* **38**, 8503-8527.

Chang, C., Ma, L. 1991. A micromechanical-based micropolar theory for deformation of granular solids. *Int. J. Solid. Struct.* **28**, 67-86.

Dafalias, Y., Papadimitriou, A., Li, X. 2004. Sand Plasticity Model Accounting for Inherent Fabric Anisotropy, *J. Eng. Mech.* **130**, 1319-1333.

Di Prisco, C., Imposimato, S. 2003. Nonlocal numerical analyses of strain localisation in dense sand. *Math. Comput. Model.* **37**, 497-506.

Di Prisco, C., Imposimato, S., Aifantis, E. 2002. A viscoplastic constitutive model for granular soils modified according to non-local and gradient approaches. *Int. J. Numer. Anal. Meth. Geomech.* **26**, 121-138.

Eringen, A. 1972. Nonlocal polar elastic continua, *Int. J. Eng. Sci.* **10**, 1-16.

Galavi, V., Schweiger, H.F. 2010. Nonlocal Multilaminate Model for Strain Softening Analysis, Int. J. Geomech. **10**(1), 30-44.

Gao, Z.W., Zhao, J.D., Li, X. 2021. The deformation and failure of strip footings on anisotropic cohesionless sloping grounds, *Int. J. Numer. Analy. Method. Geomech.* **45**, 1526-1545

Gao, Z.W., Lu, D., Du, X. 2020. Bearing Capacity and Failure Mechanism of Strip Footings on Anisotropic Sand, *J. Eng. Mech*. **146**, 04020081.

Gao, Z.W., Zhao, J.D. 2013. Strain localization and fabric evolution in sand, *Int. J. Solid. Struct.* **50**, 3634-3648.

Gao Z.W., Zhao, J.D., Li, X.S., Dafalias, Y.F. 2014. A critical state sand plasticity model accounting for fabric evolution. *Int. J. Numer. Anal. Meth. Geomech.* **38**, 370-390.

Huang, Y., Qu, S., Hwang, K. 2004. A conventional theory of mechanism-based strain gradient plasticity, *Int. J. Plast.* **20**, 753-782.

Jefferies, M. 1993. Nor-Sand: a simle critical state model for sand, *Géotechnique* **43**, 91-103.

Li, X.S., Dafalias, Y.F. 2000. Dilatancy for cohesionless soils, *Géotechnique* **50**, 449-460.

Li, X.S., Dafalias, Y.F. 2002. Constitutive Modeling of Inherently Anisotropic Sand Behavior, *J. Geotech. Geoenviron. Eng.* **128**, 868-880.

Li, X.S., Dafalias, Y.F. 2012. Anisotropic Critical State Theory: Role of Fabric, *J. Eng. Mech.* **138**, 263-275.

Loukidis, D., Salgado, R. 2011. Effect of relative density and stress level on the bearing capacity of footings on sand, *Géotechnique* **61**, 107-119.

Mallikarachchi, H., Soga, K. 2020. Post-localisation analysis of drained and undrained dense sand with a nonlocal critical state model, *Comput. Geotech.* **124**, 103572.

Mánica, M., Gens, A., Vaunat, J., Ruiz, D. 2018. Nonlocal plasticity modelling of strain localisation in stiff clays, *Comput. Geotech.* **103**, 138-150.

Oka, F., Adachi, T., Yashima, A. 1995. A strain localization analysis using a visco-plastic softening model for clay, *Int. J. Plast.* **11**, 5

Summersgill, F., Kontoe, S., Potts, D. 2017. Critical As sessment of Nonlocal Strain-Softening Methods in Biaxial Compression, *Int. J. Geomech.* **17**, 04017006.

Summersgill, F., Kontoe, S., Potts, D. 2018. Stabilisation of excavated slopes in strain-softening materials with piles, *Géotechnique* **68**, 626-639.

Tejchman, J., Wu, W. 2010. FE-investigations of micro-polar boundary conditions along interface between soil and structure, *Granul. Matter*. **12**, 399-410.

Tian, Y., Yao, Y.P. 2017. Modelling the non-coaxiality of soils from the view of cross-anisotropy, *Comput. Geotech.* **86**, 219-229.

Tordesillas A, Walsh D (2002) Incorporating rolling resistance and contact anisotropy in micromechanical models of granular media. *Powder Technol.* **124**, 106–111.

Yao, Y.P., Liu, L., Luo, T., Tian, Y., Zhang, J.M. 2019. Unified hardening (UH) model for clays and sands, *Comput. Geotech.* **110**, 326-343.

Yao, Y.P., Wang, N., Chen, D. 2020. UH model for granular soils considering low confining pressure. Acta Geotech

Yao, Y.P., Tian, Y., Gao, Z.W. 2017. Anisotropic UH model for soils based on a simple transformed stress method, *Int. J. Numer. Anal. Meth. Geomech.* **41**, 54-78

Zhao, J.D., Sheng, D.C., Rouainia, M., Sloan, S.W. 2005. Explicit stress integration of complex soil models, *Int. J. Numer. Analy. Method. Geomech.* **29**, 1209-12